NASA CR-134616

Vol I N74-19345
Vol II 39723

Department of Aerospace Engineering

University of Cincinnati

EROSION IN RADIAL INFLOW TURBINES - VOLUME II

BALANCE OF CENTRIFUGAL AND RADIAL DRAG FORCES ON EROSIVE PARTICLES

By:

W.B. Clevenger, Jr.

and

W. Tabakoff

(NASA-CR-134616) EROSION IN RADIAL INFLOW TURBINES. VOLUME 2: BALANCE OF CENTRIFUGAL AND RADIAL DRAG FORCES ON EROSIVE PARTICLES Final (Cincinnati Univ.) ~~37~~ 36 p HC $5.00 CSCL 21E G3/28

N74-30238

Unclas 39723

Supported by:

NATIONAL AERONAUTICS AND SPACE ADMINISTRATION

Lewis Research Center

Contract NGR 36-004-055

1. Report No.	2. Government Accession No.	3. Recipient's Catalog No.
NASA CR 134616		

4. Title and Subtitle	5. Report Date
EROSION IN RADIAL INFLOW TURBINES-VOLUME II: BALANCE OF CENTRIFUGAL AND RADIAL DRAG FORCES ON EROSIVE PARTICLES	April 1974
	6. Performing Organization Code
7. Author(s)	8. Performing Organization Report No.
W.B. Clevenger, Jr. and W. Tabakoff	
	10. Work Unit No.
9. Performing Organization Name and Address	11. Contract or Grant No.
Department of Aerospace Engineering University of Cincinnati Cincinnati, Ohio 45221	NGR 36-004-055
	13. Type of Report and Period Covered
12. Sponsoring Agency Name and Address	
National Aeronautics and Space Administration Washington, D.C. 20546	14. Sponsoring Agency Code

15. Supplementary Notes

Final Report. Project Manager, Jeffrey E. Haas, Fluid Systems Components Div., NASA, Lewis Research Center, Cleveland, Ohio 44135

16. Abstract

This report considers the particle motion in two-dimensional free and forced inward flowing vortices. A particle in such a flow field experiences a balance between the aerodynamic drag forces that tend to drive erosive particles toward the axis, and centrifugal forces that prevent these particles from traveling toward the axis. The results predict that certain sizes of particles will achieve a stable orbit about the turbine axis in the inward flowing free vortex. In this condition, the radial drag force is equal to the centrifugal force. The sizes of particles that will achieve a stable orbit is shown to be related to the gas flow velocity diagram at a particular radius. A second analysis yields a description of particle sizes that will experience a centrifugal force that is greater than the radial component of the aerodynamic drag force for a more general type of particle motion.

17. Key Words (Suggested by Author(s))	18. Distribution Statement
Radial Turbine Erosion Particle Dynamics Particulated Flow	Unclassified - Unlimited

19. Security Classif. (of this report)	20. Security Classif. (of this page)	21. No. of Pages	22. Price*
Unclassified	Unclassified	35	$3.00

*For sale by the National Technical Information Service, Springfield, Virginia 22151

NASA-C-168 (Rev. 6-71)

NASA CR-134616

EROSION IN RADIAL INFLOW TURBINES - VOLUME II

BALANCE OF CENTRIFUGAL AND RADIAL DRAG FORCES ON EROSIVE PARTICLES

By:

W.B. Clevenger, Jr.

and

W. Tabakoff

Supported by:

NATIONAL AERONAUTICS AND SPACE ADMINISTRATION

Lewis Research Center

Contract NGR 36-004-055

TABLE OF CONTENTS

SUMMARY

Particle motion in two-dimensional free and forced inward flowing vortices was studied. A balance exists between the aerodynamic drag forces that tend to drive erosive particles into radial inflow turbines, and the centrifugal forces that can prevent these particles from passing through the turbine. The radial motion of the particles is then determined by comparison of the radial components of the aerodynamic drag and centrifugal forces.

When the radial motion is zero, particles achieve a stable orbit about the turbine axis in the inward flowing free vortex. In this condition the radial drag force is equal to the centrifugal force. The sizes of particles that will tend to achieve a stable orbit is shown to be related to the gas flow velocity diagram at a particular radius. The characteristic length, a similarity parameter which relates the particles that follow the same trajectory in equivalent flow fields is used to describe the particle sizes that will tend to orbit the axis.

A second analysis is presented to describe more realistically the particle motion as it enters the free vortex. This study yields a description of particle sizes in terms of a characteristic length, that will probably not penetrate the radial turbine rotor.

INTRODUCTION

The purpose of this study is to investigate the erosion phenomena in radial inflow turbines and to study ways of eliminating this erosion. The overall study includes an investigation of erosive particle trajectory similarity, investigation of the balance between radial aerodynamic drag and centrifugal forces acting on the particles, a review of the phenomena of erosion of blade materials by the action of particles, and an investigation of the trajectories that particles follow as they pass through a radial inflow turbine. The results of these investigations will be published in a series of five volumes which will cover the indicated topics, with the fifth volume presenting the numerical programs that were developed. This report considers the second topic.

In recent times, the problem of particle erosion has become important due to the significant decreases in the rated operating lifetimes and performance of gas turbine engines which are used in dusty environments. The most significant affects of erosion have been observed on active military helicopters, where operations at low altitudes and remote landing fields have greatly increased the number of particles that enter the engines. Although these helicopters have main engines which utilize axial flow turbines, some also have auxiliary engines used as power sources for special devices which utilize radial turbines, as shown schematically in Figure 1.

Radial inflow turbines have also been used on small portable power plants which are also likely to be used in areas where dust ingestion will occur. In addition, radial inflow turbines have long been used in turbochargers on reciprocating engines. In heavy construction equipment, such engines are used in very dusty environments where ingested dust and sand may not necessarily be removed from the air before entering the turbine. Finally, radial inflow turbines are seriously being considered for future use in transportation vehicles such as trucks, buses, and automobiles. These engines will at times have incomplete filtering of incoming air, leading to the ingestion of erosive size particles that could

seriously threaten the future performance of the engine.

These radial turbine engines have, however, a more serious erosion problem than axial flow turbines. In radial turbines, the larger particles experience a radially outward centrifugal force that is greater than the radially inward component of the aerodynamic drag force. In the axial flow turbine, the centrifugal force acts perpendicular to the aerodynamic drag force. Thus, in radial turbines most particles are prevented from passing through the rotor and strike the trailing edges fo the stators and the leading edges of the rotor many times. In axial flow turbines, the particles generally move outward to the tip region, but all particles have a tendency to pass out of the turbine.

By studying the force balance on the particles a better understanding of the movement of the particles in the radial turbine will be gained. Also, such an analysis will yield a measure of the sizes of particles that can be expected to cause serious erosion problems.

There have been several reports published which give results that will be useful for comparison purposes in this report. Volume I of this series of reports (1) explains the derivation and applicability of a parameter which allows particles used in cold flow turbines and cascades to be defined such that their trajectories will be similar to those of real particles in equivalent hot flow turbine applications.

In addition, Reference 2 describes the results of a test program that was performed to relate the decrease in engine operating lifetime to the amount and sizes of particles that enter the turbine. These studies indicate that particles as small as 2 to 3 microns can still be expected to cause a serious decrease in the engine operating lifetime.

Reference 3 also reports the results of an experimental effort to study the erosion in radial turbines. The study describes several design modifications that were performed to hopefully reduce the seriousness of the erosion that occurred, however, the

authors indicate that the modifications were only slightly successful.

ANALYSIS AND RESULTS

Characteristic Length

As indicated above, Reference 1 describes the derivation and applicability of a similarity parameter that allows particles which follow a certain trajectory in a real gas turbine to be related to a particle that will follow the same trajectory in an equivalent cold gas turbine. The similarity parameter is a characteristic length and is given by the following equation

$$\delta = \frac{10}{3} \frac{\rho_p D_p}{\rho_g} \tag{1}$$

This similarity parameter, which results from the matching of the inertial and drag forces acting on a particle, is derived in Reference 1.

The characteristic length is a useful parameter because it allows the grouping of several variables that influence the trajectory of a particle into a single term. This allows a much wider range of applicability of the trajectory data and allows the use of data from equivalent cold flow turbines and cascade tunnels.

In the subsequent derivations in this report, the variables can be grouped to determine the characteristic lengths which will have special significance according to the principles used in the derivation.

Vortex Flow

The gas flow regions of interest in this study are the region just before the rotor inlet which is a free inward flowing vortex, and the region just inside the rotor tip, which has the characteristics of a forced inward flowing vortex. In this report, the change from the free to the forced vortex flows is assumed to occur

instantaneously at the tip. In reality, there is a smooth transition from the free to the forced vortex flows that begins at the rotor tip and is usually completed at approximately 0.8 times the tip radius.

Both of these flow fields are well defined for compressible gas flows and are described by relatively straightforward analytical techniques.

Figure 2 shows the coordinate system that will be used throughout this report. The radius, r, is measured from the axis of the turbine rotor. The regions of interest in this report are between 0.5 and 1.5 times the rotor tip radius. Although the actual flow fields are limited to a much smaller region, the larger area of the analytical study will provide greater insight into the phenomena of particles moving outward away from the axis. A two-dimensional flow pattern is assumed to exist throughout the flow region and angular symmetry is also assumed, eliminating effects caused by distortion of the flow into the rotor.

The free vortex is defined by the fact that for conservation of angular momentum, the term

$$\lambda = V_u \, r = \text{constant} \tag{2}$$

must be constant everywhere within the flow field. With the tangential velocity known at any particular radius, then λ is determined and can be used to find the tangential velocity at any other radius.

The radial velocity of the gas flow in the free vortex can be found from the continuity equation

$$\dot{w} = -\rho_g \, V_r \, A \tag{3}$$

The minus sign in Equation (3) results from the fact that the radial component of velocity is usually assumed to be positive when in the increasing r direction. Because the vortex flow in this case is inward, the minus sign is added to give a positive

mass flowrate. Because the gas density in this expression varies with the velocity, isentropic flow is assumed and the following relationship is obtained.

$$\rho_g = \rho_{t_g} \left[1 - \frac{\gamma-1}{\gamma+1} \left(\frac{V}{V_{cr}}\right)^2\right]^{\frac{1}{\gamma-1}} \tag{4}$$

where

$$V = \sqrt{V_r^2 + V_u^2} \tag{5}$$

is used to completely define the gas properties at any location within the free vortex.

In the forced vortex, the analysis of the fluid flow problem follows much the same pattern as in the previous case, but with added complexity which occurs because the rotor wheel removes work energy from the gas, thus causing the stagnation temperature of the gas to decrease.

The rotation of the wheel is given by

$$\omega = \frac{U}{r} \tag{6}$$

where ω is a constant. Usually a radial inflow turbine has a tangential component of relative velocity near the tip, but in this analytical solution this will be neglected and based on this assumption $V_u = U$. Equation (6), with V_u inserted for the wheel speed allows the determination of the tangential velocity of the gas at any radius.

As in the previous case, the continuity equation takes the form given in Equation (3).

The added complexity of the rotor flow now becomes apparent because this gas flow has a stagnation temperature that is not constant with the radius, and thus, the stagnation gas density and critical velocities in Equation (4) are also functions of the radius.

This relationship can be determined from the expression relating the stagnation temperature and the change in the whirl of the gas, which is

$$T_t - T_{t_{tip}} = \frac{V_u U - (V_u U)_{tip}}{g\, C_p} \tag{7}$$

This equation reflects the fact that the conditions at the rotor tip have been arbitrarily selected as the known reference values. Assuming $U = V_u$ within the rotor, then Equation (7) can be written as

$$T_t = T_{t_{tip}} \left[1 + \frac{V_u^2 - V_{u_{tip}}^2}{g\, C_p\, T_{t_{tip}}}\right] \tag{8}$$

Because V_u varies with r according to the expression given in Equation (6), Equation (8) gives the stagnation temperature variation with r.

Even though there is a variation in the stagnation conditions within the forced vortex, the flow is still assumed to be isentropic. Therefore, the stagnation density at any radius can be related to the stagnation temperature by

$$\frac{\rho_t}{\rho_{t_{tip}}} = \left(\frac{T_t}{T_{t_{tip}}}\right)^{\frac{1}{\gamma-1}} \tag{9}$$

Finally, Equation (4) can be applied at a specific point within the flow field to determine the gas density. The critical velocity required in this equation is given by

$$V_{cr} = \sqrt{\frac{2g\gamma}{\gamma+1} RT_t} \tag{10}$$

where the stagnation temperature, T_t, is given by Equation (8).

With the gas flow in both the free vortex and the forced vortex determined, it becomes necessary to note that these two flows must match at the tip radius. For the purposes of illustration, the conditions at the tip of a typical radial inflow turbine were selected as the flow field to be used in this investigation. Figure 3a indicates the angle and magnitude of the air flow, which was taken to have standard sea level stagnation conditions at the rotor tip. The particular rotor tip value was 7.521 cm which was arbitrarily selected as a typical value for a radial turbine rotor.

Figure 3b shows the most general case of the motion of a particle and the motion of the gas at a particular radius. The particle will usually move in the same general direction as the gas, but both the magnitude and velocity direction will tend to lag the gas velocity.

Because the gas density varies with the radial position from the nozzle exit through the rotor, the characteristic length, given in Equation (1) will also tend to change with the radius. Figure 4 indicates this variation in characteristic length for natural quartz sand particles, Silicon Dioxide, of 0.5 micron size in cases where the flow is completely free vortex or forced vortex types. Generally, the free vortex exists in the flow region where the radius ratio (r/r_{tip}) is greater than one, and the forced vortex exists in the flow region where the radius ratio (r/r_{tip}) is less than one, although there is a smooth transition from the free vortex to the forced vortex near the leading edge of the rotor. In the curves that follow, this smooth transition is omitted and a cusp occurs at the location where the two flow fields meet. This cusp occurs at the radius corresponding to the rotor tip.

Forces Acting on the Particle

With the motion and properties of the gas flow understood, the action of this gas on the motion of a particle can be determined. This action is in the form of an aerodynamic drag force

that acts on the particle and tends to accelerate the particle radially inward. Newton's Law relates the motion of the particle and the forces that act on it with the expression

$$\bar{D} = m\bar{a}$$

It should be noted that both drag and acceleration are vector quantities.

Based on Figure 3b, the drag force acting on the particle can be written,

$$\bar{D} = \frac{1}{2} \rho_g \bar{V}^2 A_p C_D \left[\frac{(V_g)_r - (V_p)_r}{|\bar{V}|} \bar{e}_r + \frac{(V_g)_u - (V_p)_u}{|\bar{V}|} \bar{e}_\theta \right. \tag{12}$$

Because the centrifugal force will act only in the radial direction, the radial component of the drag force is the component that must be considered. Using the fact that $(V_g)_r = V_g \cos \beta_g$ and $(V_p)_r = V_p \cos \beta_p$, the radial component of the drag force is

$$D_r = \frac{1}{2} \rho_g \bar{V}^2 A_p C_D \left[\frac{V_g \cos \beta_g - V_p \cos \beta_p}{|\bar{V}|}\right] \tag{13}$$

This radial drag force will tend to drive the particle through the vortex regions near the rotor tip. The centrifugal force, on the other hand, will tend to drive the particles radially outward against the gas flow. This centrifugal force is given by

$$F = \frac{m(V_p)_u^2}{r} = \frac{m V_p^2 \sin^2 \beta_p}{r} \tag{14}$$

where the tangential velocity of the particle has been expressed as $(V_p)_u = V_p \sin \beta_p$.

The condition that is satisfied when the particles tend to accelerate outward is that the centrifugal force must be greater than the radial drag force

$$F > D_r \tag{15}$$

This expression applies to particles that are moving inward and are experiencing a radial deceleration, and particles that are moving outward and are experiencing a radial acceleration.

Substitution of Equations (13) and (14) into the inequality indicated by Equation (15), and assuming that the particles are spherical with constant drag coefficient of 0.4, yields the condition that must be satisifed by the particle if it is to accelerate outward.

$$\frac{\delta}{r} > |\bar{V}| \frac{V_g \cos \beta_g - V_p \cos \beta_p}{V_p^2 \sin^2 \beta_p} \tag{16}$$

When the value of the particle characteristic length is greater than the term on the right hand side of Equation (16), the particle will accelerate radially outward.

It should be noted that most sand and dust particles are not spherical in shape. However, consideration of nonspherical particles requires addition of lift and moment forces on the particle, and these forces, as well as the drag forces would tend to flucuate with time in a random manner, depending on the particle orientation. The value of drag coefficient would probably increase, with values as great as three times the values for the spherical particle. In addition, the constantly changing particle surface area would also have an influence on the particle acceleration. This variation would of course depend on the nature of the particle shape.

Reference 4 presents some experimental results of the affect of nonspherical particles accelerating in a fully developed flow. The data indicates an approximately normal distribution of particle

velocities about the velocity which is predicted assuming spherical particles. The standard deviation of this data is about 10% of the predicted velocity.

Using Equation (16), several special cases can be studied which illustrate the phenomena that occurs as the particle passes through the radial turbine. These special cases illustrate the phenomena that occur and provide information that allow a more thorough presentation of the results of subsequent volumes of this report.

Case 1. Particle in Orbit About Axis

In this particular example, the particle will orbit the axis at some constant radius. At this equilibrium radius, a steady state condition will be reached with the particle accelerating to a velocity vector that is equal in magnitude and direction to the tangential component of the gas velocity. Figure 5 contains the combined gas flow, particle velocity diagram for such a case. In this particular example

$$\beta_p = \pi/2$$

$$V_p = (V_g)_u = V_g \sin \beta_g$$

$$|\bar{V}| = |\bar{V}_g - \bar{V}_p| = |(\bar{V}_g)_r| = V_g \cos \beta_g \qquad (17)$$

Substitution of these into Equation (16) yields

$$\delta > \delta_o \qquad (18)$$

where

$$\delta_o = \frac{r}{\tan^2 \beta_g} \qquad (19)$$

Equation (18) expresses the requirement that for outward acceleration of the particle the characteristic length, δ, which is primarily a property of the particle, must be greater than the value of δ_o, the orbit characteristic length, which is primarily a property of the gas flow.

The fluid solution provides the gas velocity vector direction β_g, as the gas goes through the free and forced vortex. This can be used to determine the variation in the orbit characteristic length with the radius changes. Figure 5 indicates this variation and shows the cusp point that occurs when the fluid flow changes from the free to forced vortex. Because the orbit characteristic length, δ_o, is independent of the particle diameter, one curve will apply to all particles.

Figure 6 shows the combination of Figures 4 and 5, and is included to illustrate the phenomena of a particle at equilibrium. At the equilibrium radius, the particle will rotate about the axis with a velocity equal to the tangential velocity of the gas. The particle will have no radial velocity component in the steady state condition. If the particle experiences a disturbance that makes its radius slightly larger, than δ will be less than δ_o, and the particle will experience a larger drag force that pushes it back toward the equilibrium radius. If the particle experiences a disturbance that makes its radial position slightly smaller, then the particle will experience a slightly larger centrifugal force that will tend to drive it back toward the equilibrium radius.

Finally, Figure 7 shows the variation in characteristic length with radius for particles of many different sizes. The figure indicates that all particles having diameters less than about 0.48 microns will not have an equilibrium radius within the flow field, but will pass through the free vortex and forced vortex unhindered. Particles having diameters greater than about 0.48 microns, however, will have a tendency to establish an orbit about the axis at the equilibrium radius.

The velocity diagram used to describe the motion of a particle at the equilibrium radius is restricted to a very special case

where the particle has been accelerated to the tangential velocity of the gas. A more general approach would be to consider the forces acting on a particle that moves in the same general direction of the gas, but with a velocity that is less than the gas velocity. Because all particles will tend to accelerate more slowly than the gas, an approach such as this would better describe the motion of the particles as they enter the vortex regions.

Case 2. Particle Lags Gas Velocity

Figure 8 contains the velocity diagram of the gas and particle in this particular case. In this case,

$$\beta_p = \beta_g = \beta$$

$$V_p = \zeta V_g \quad \text{where} \quad 0 < \zeta \leq 1.0$$

$$|\bar{V}| = |\bar{V}_g - \bar{V}_p| = V_g - V_p \tag{20}$$

Equation (16) then becomes

$$\delta > \delta_L \tag{21}$$

where δ_L is called the limit characteristic length and is given by

$$\delta_L = \frac{(1 - \zeta)^2}{\zeta^2} \frac{r \cos \beta}{\sin^2 \beta} \tag{22}$$

As in the previous example, a particle will accelerate radially outward if its characteristic length, δ, is greater than δ_L.

Figure 8 also shows the variation of the limit characteristic length, δ_L, as the radius changes in both free vortex and forced vortex types of flow for a particle that lags the gas velocity by 50%. As in the previous cases, the real limiting curve will be a

combination of the free vortex and forced vortex variations. The dashed line indicates the approximate uniform variation that can be expected just inside the rotor.

Combining the correct parts of the two curves given in Figure 8, with similar curves corresponding to different velocity lags, yields a family of limit curves which are shown in Figure 9. Included in this figure is the family of curves that indicate the variation in the characteristics length with radial location for different size particles. Of special interest is the fact that the particles with diameters of about 2 microns and having 50% velocity lag will be the smallest that experience a centrifugal force that is greater than the inward directed drag force. Although this is in agreement with the experimental results presented in Reference 2, the restrictions on the particle motion, that is, the particle restricted to motion in the same direction as the gas and with a velocity of 50% of the gas velocity, is without foundation and was used here because the assumption yielded a worthwhile analytical result. Volume III of this series of articles will consider the trajectories of particles in the radial inflow turbine, and will consider the values of ζ and particle velocity direction at all locations of a realistic turbine.

Case 3. General Particle Motion at a Particular Radius

Although a particle will not in general remain at a particular radius, consideration of the variations in the terms on the right hand side of Equation (16) will provide some understanding of the trends in particle radial acceleration as the particle velocity vector varies away from the gas velocity vector. Figure 3b illustrates this general case. In this particular study, the velocity diagram at the rotor tip was selected as the gas flow. When this is done, the quantities V_g, β_g and r become constants and the quantities V_p and β_p are the independent variables.

The terms on the right hand side of Equation (16) can be grouped together to form a dependent variable Λ given by

$$\Lambda = \frac{|\bar{V}| \ (V_g \cos \beta_g - V_p \cos \beta_p)}{V_p^2 \sin^2 \beta_p} \qquad (23)$$

Figure 10 shows the variation in this function that occurs when the particle velocity is maintained at 50% of the gas velocity while β_p varies from 0 to 90°.

The point on this curve indicated by the circle corresponds to the condition illustrated in Case 2, where the velocity lag was 50% and the particle had a velocity direction corresponding to the direction of the gas velocity.

In order to interpret this figure, it must be realized that for a particular particle to accelerate outward, the condition that must be satisfied is

$$\frac{\delta}{r} > \Lambda \qquad (24)$$

Thus, any particle satisfying conditions of 50% velocity lag, β_g and δ such that when plotted on the figure the point representing this particle lies above the curve, then this particle will accelerate radially outward.

It should be noted that all particles that have velocity angles less than 61% and velocity magnitudes 50% of the gas velocity will always accelerate radially outward. This occurs because the restriction of the particle velocity to a constant value causes the radial particle velocity component to exceed the radial gas velocity component. When this happens, the radial component of the aerodynamic drag force acts in the outward direction. Such motion could possibly occur because of particle impacts on the stator blades.

Figure 11 shows the function Λ plotted versus β_p, with ζ as a parameter. As in the previous figure, the point indicated by the circle represents the special Case 2, where $\beta_p = \beta_g$ and $\zeta = 50\%$. The point indicated by the square represents the special Case 1 where $\beta_p = 90°$ and $\zeta = \sin 75.8° = 0.969$.

The figure illustrates the fact that most particles experience forces that tend to push them radially outward. At a particular radius, the motion of some very small particles will be such that they will experience radial forces pushing them inward, but this is possible only for very special particle motion direction.

DISCUSSION OF RESULTS

The phenomenon that prevents particles from penetrating the vortex region of a radial inflow turbine is the cause of significant amounts of erosion in the turbine. The usefulness of the analysis presented in this report lies in the ability to determine, based on the characteristics of the turbine design, the sizes of particles that must be removed from the vortex regions of the radial inflow turbine.

The orbit characteristic length, δ_o, based on the rotor tip radius, represents the lower limit of particle sizes that might fail to penetrate the vortex regions. Particles with characteristic lengths smaller than δ_o can be expected to penetrate the vorticies at all times. Particles with characteristic lengths greater than the orbit characteristic length based on the rotor tip radius will always have a tendency to experience an outward acceleration.

It should be noted that this analysis has not considered the affect of blade thickness in the rotor. However, the results presented concerning the equilibrium radius and the orbit characteristic length will not be influenced by the addition of the blade thickness because the equilibrium radius occurs only in the free vortex part of the flow, where there are no rotor blades. The inclusion of the blade thickness will cause the gas density in the rotor to decrease slightly because of a blockage effect. This will cause a slight shifting of the variation of characteristic lengths with radius in the rotor, but it is not expected to significantly change the trends that are indicated here.

For the particular combination of rotor size and velocity diagram considered in this report, a particle having a characteristic length less than 0.48 cm can be expected to always penetrate the vortex regions. This corresponds to a sand particle (SiO_2) having a diameter of approximately 0.48 microns.

The previous results indicate only the size of particles that can always be expected to penetrate the vortex regions of the turbine. Larger particles may also penetrate the vortex regions because of the nature of their velocity and direction as they enter the free vortex. For example, according to the results in Figure 9, particles with characteristic lengths of about 2.0 cm and restricted to having a velocity greater than 50% of the air velocity and always moving in the same direction as the air velocity will not experience centrifugal forces greater than the radial component of the aerodynamic drag force. Thus, particles of this size and satisfying these conditions will penetrate the vortex flows. This characteristic length corresponds to a typical sand particle having a diameter of about 2 microns.

Although this is in agreement with the results presented in Reference 2, the restrictions on the particle motion is without foundation and requires further study as explained previously. A subsequent volume of this report will consider the trajectories of particles as they penetrate all the gas flow regions of the radial turbine. That volume will study the nature of the velocity diagrams of gas flow and particle flow and draw a more complete conclusion of the sizes and characteristics of particles that will not penetrate the radial turbine rotor.

CONCLUSIONS

The forces that influence the motion of a particle as it passes through the vortex regions of a radial inflow turbine are considered. These forces are primarily the radial component of the aerodynamic drag force and the centrifugal force. By balancing these two forces, the phenomena that prevents particles from penetrating the vortex

regions is demonstrated.

Consideration of the forces acting on a particle that orbits the axis demonstrates that such a motion is theoretically possible. Such a particle will orbit the axis at an equilibrium radius, and will not tend to move radially inward or outward. Small disturbances in the particle motion causes forces that tend to push the particle back to the original equilibrium radius.

Consideration of the forces acting on particles which have the same direction as the air velocity, which is a more realistic representation of the motions of particles as they enter the vortex regions, demonstrates that even larger particles will experience radial acceleration away from the axis. Such particles are of the size that cause severe erosion in radial inflow turbines.

Consideration of the more general motion of particles at a particular radius illustrates the size of particles that can be expected to always penetrate the vortex regions and the sizes of particles that will probably never penetrate the vortex region.

REFERENCES

1. Clevenger, W.B., Jr., and Tabakoff, W., "Erosion in Radial Inflow Turbines - Volume I: Erosive Particle Trajectory Similarity," prepared for NASA, Lewis Research Center, January 1974.
2. Montgomery, J.E. and Clark, J.M., Jr., "Dust Erosion Parameters for a Gas Turbine," SAE Paper No. 538, June 1962.
3. Shoemaker, H.E. and Shumate, C.P., "Techniques for Reducing Sand and Dust Erosion in Small Gas Turbine Engines," SAE Paper No. 700706, September 1970.
4. Grant, G. and Tabakoff, W., "A Quasi-Analytical Method for the Calculation of Particle Trajectories," University of Cincinnati, Department of Aerospace Engineering Report No. 73-35, February 1973.

LIST OF SYMBOLS

A	Cross-sectional area of the particle - meter^2
C_D	Drag Coefficient
C_p	Specific heat at constant pressure - joule/kilogram °K
$\bar{D}$	Drag vector - newtons
D	Particle diameter - meters
$\bar{e}_r, \bar{e}_\theta$	Unit vectors in the polar coordinate system
F	Centrifugal force - newtons
g	The acceleration of gravity - meters/second^2
r	Coordinate measured from the axis - meters
T	Temperature, °K
U	Wheel speed - meters/second
$\|\bar{V}\|, V$	Velocity - meters/second
$\dot{w}$	Mass flowrate - kilogram/second
β	Angle of velocity vector, measured from the r-coordinate
γ	Ratio of specific heats
δ	Characteristic length - meters
λ	Prerotation of the gas - meters^2/second
ρ	Density - kilograms/meter^3
ζ	Velocity ratio - V_g/V_p
Λ	Function given in Equation (23)

Subscripts

cr	Represents property evaluated at critical conditions
g	Represents gas property
L	Used to denote limit characteristic length

o	Used to denote orbit characteristic length
p	Represents particle property
r	Represents component in the radial direction
t	Used to denote stagnation gas properties
tip	Property evaluated at the rotor tip
u	Represents component in the tangential direction

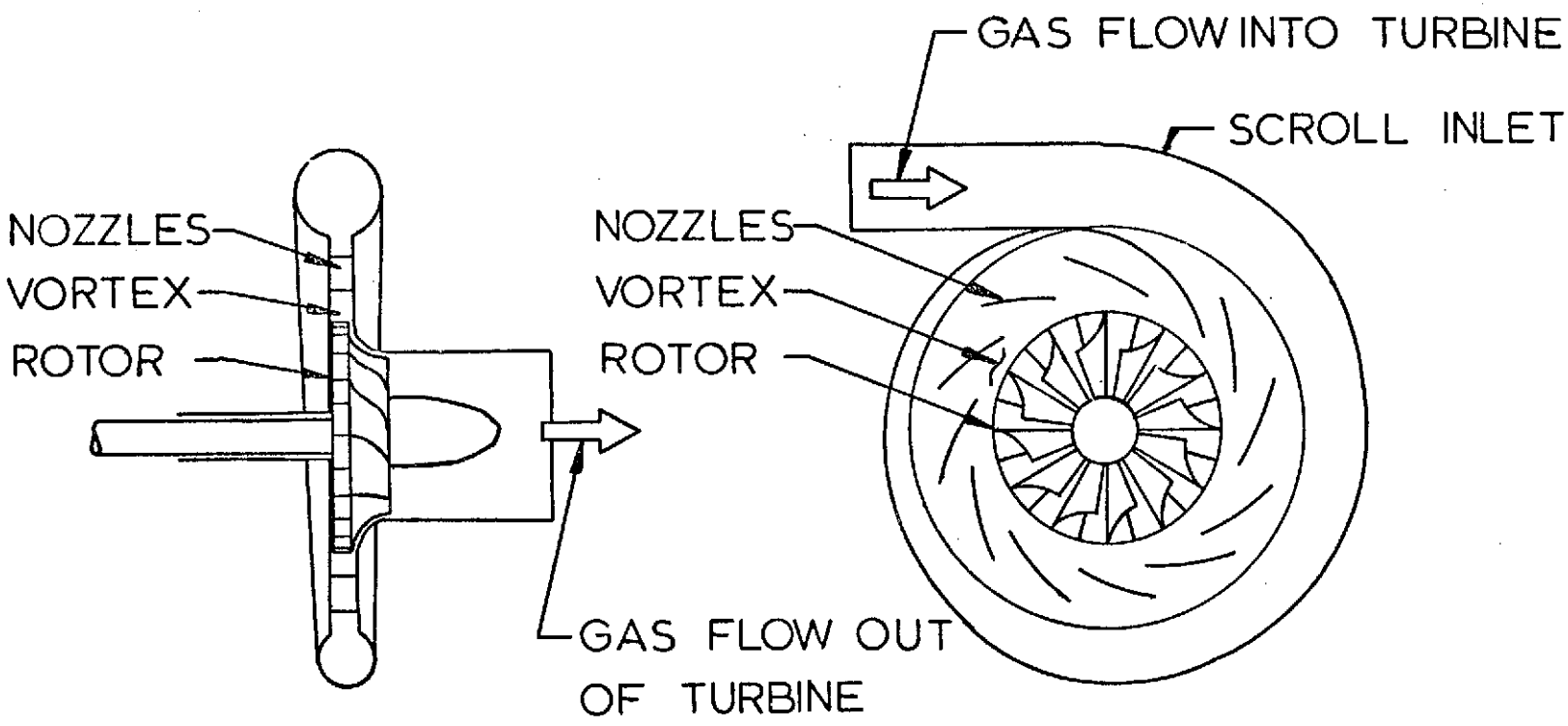

FIGURE 1. SCHEMATIC OF TYPICAL RADIAL INFLOW TURBINE

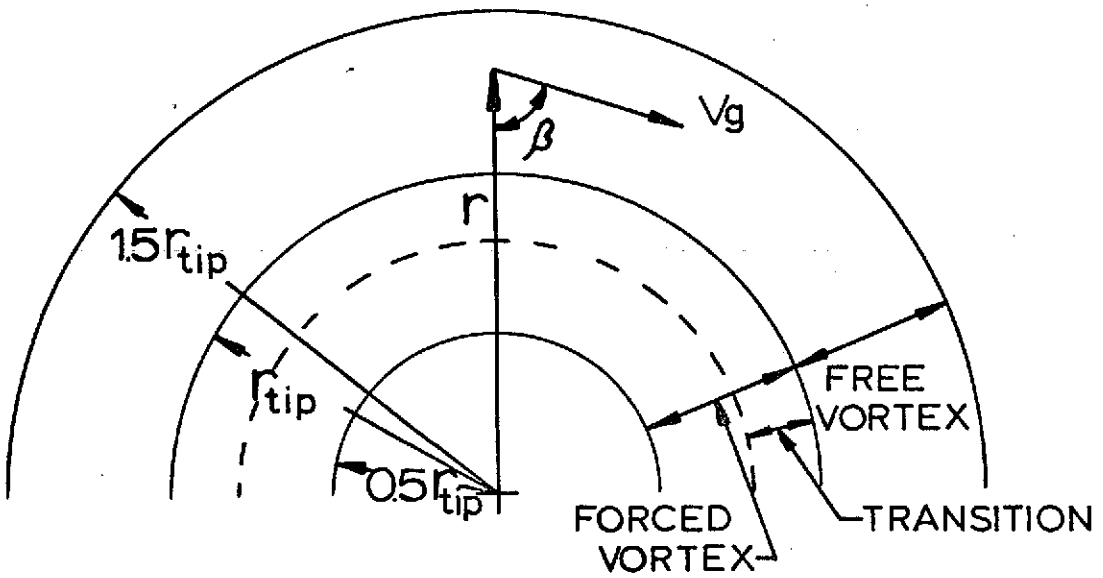

FIGURE 2. COORDINATE SYSTEM

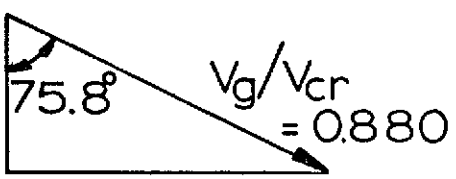

(a) Gas Diagram at Rotor Tip

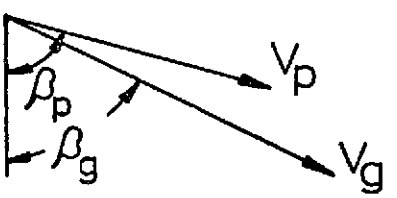

(b) Combined gas particle diagram

FIGURE 3. VELOCITY DIAGRAMS

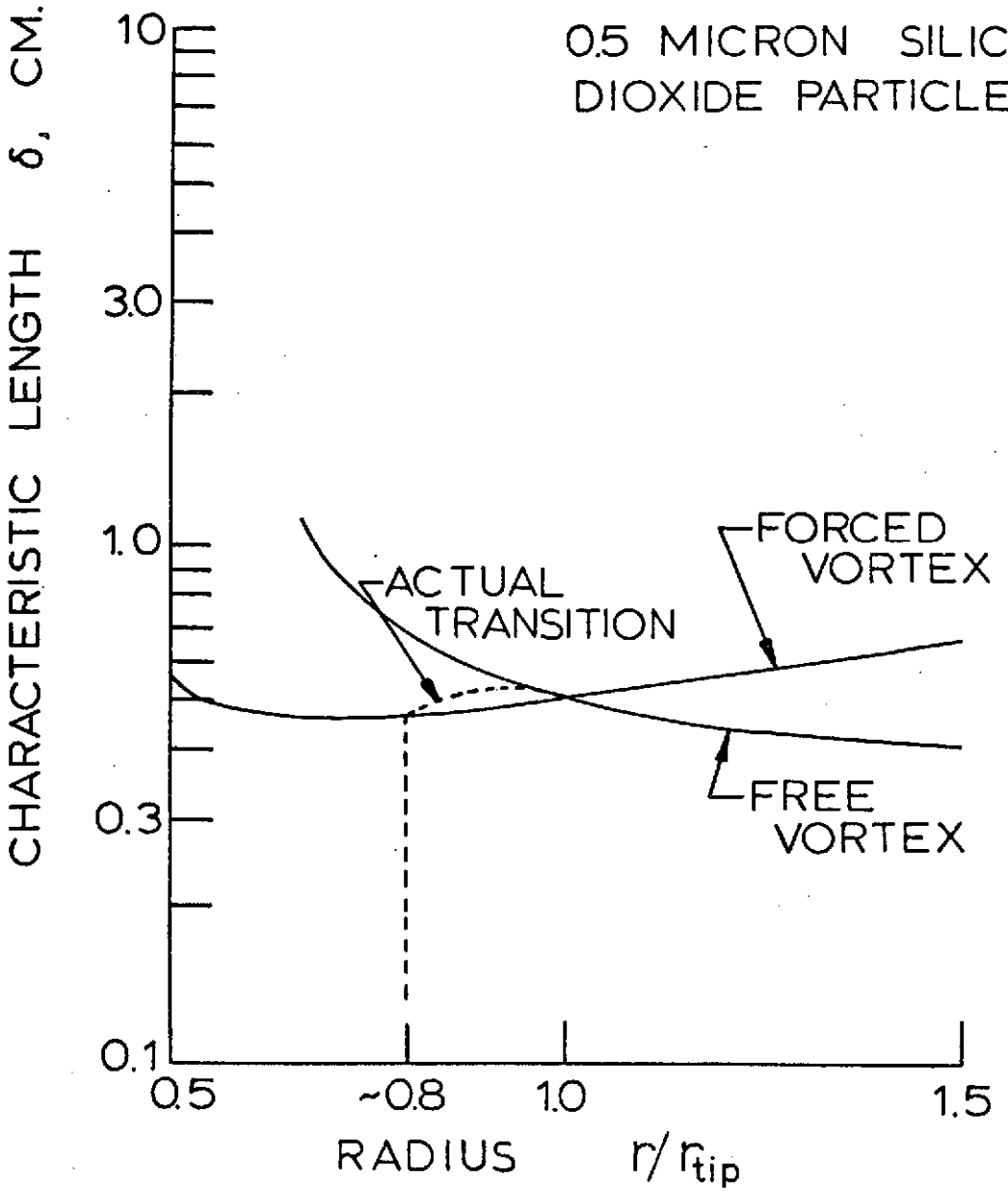

FIGURE 4. VARIATION IN CHARACTERISTIC LENGTH WITH RADIUS

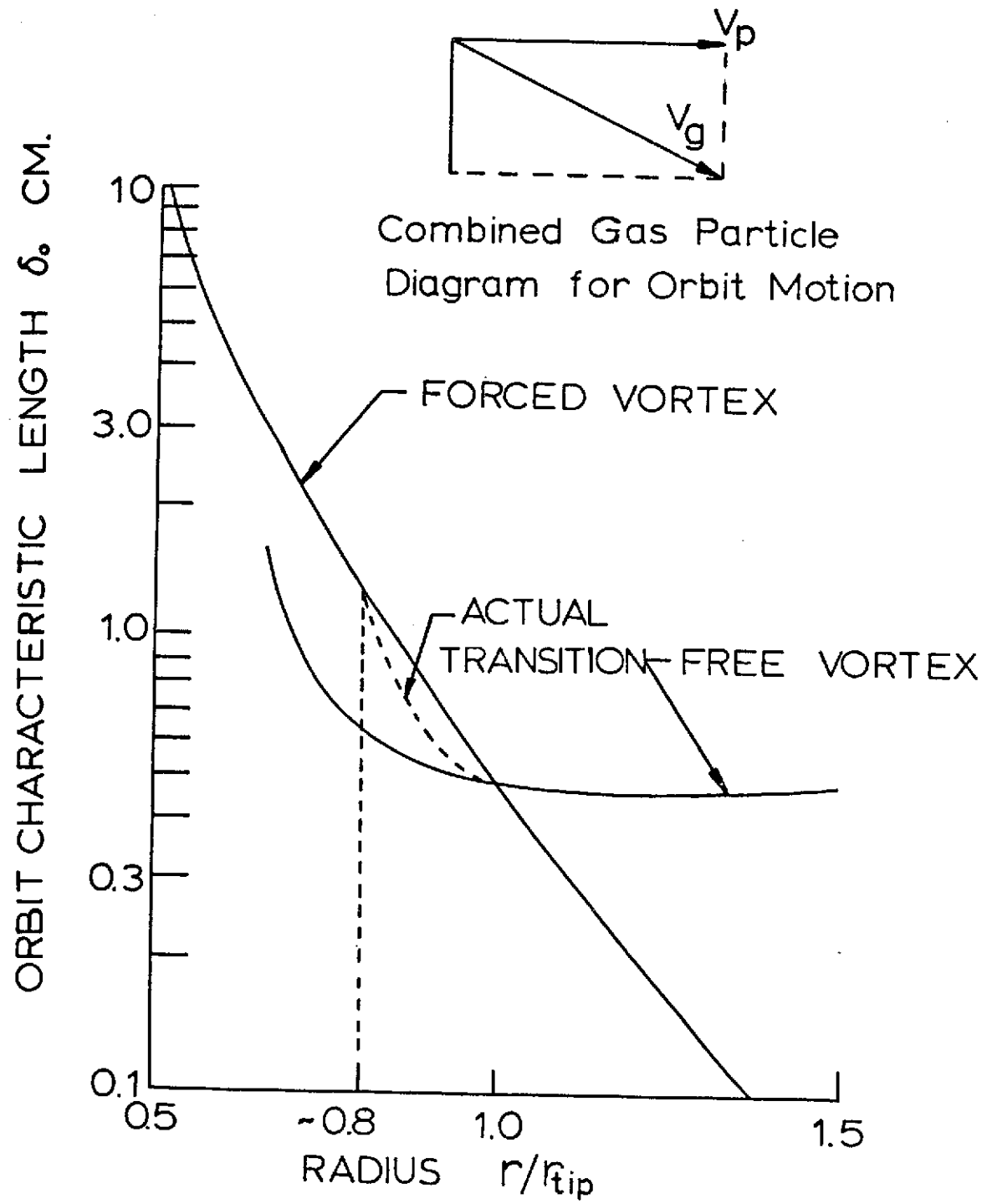

FIGURE 5. ORBIT CHARACTERISTIC LENGTH VARIATION WITH RADIUS

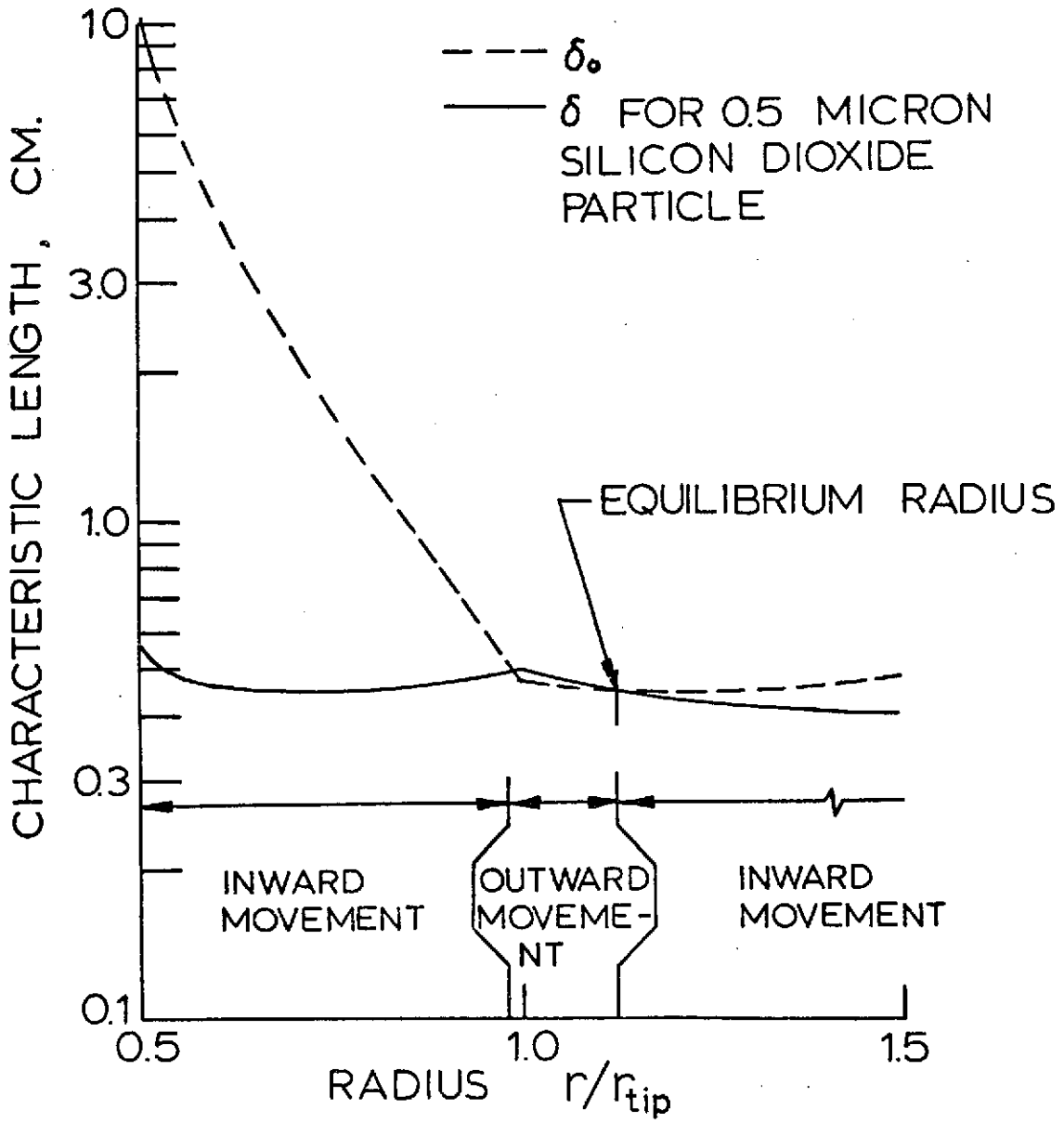

FIGURE 6. CHARACTERISTIC LENGTH VARIATION WITH RADIUS

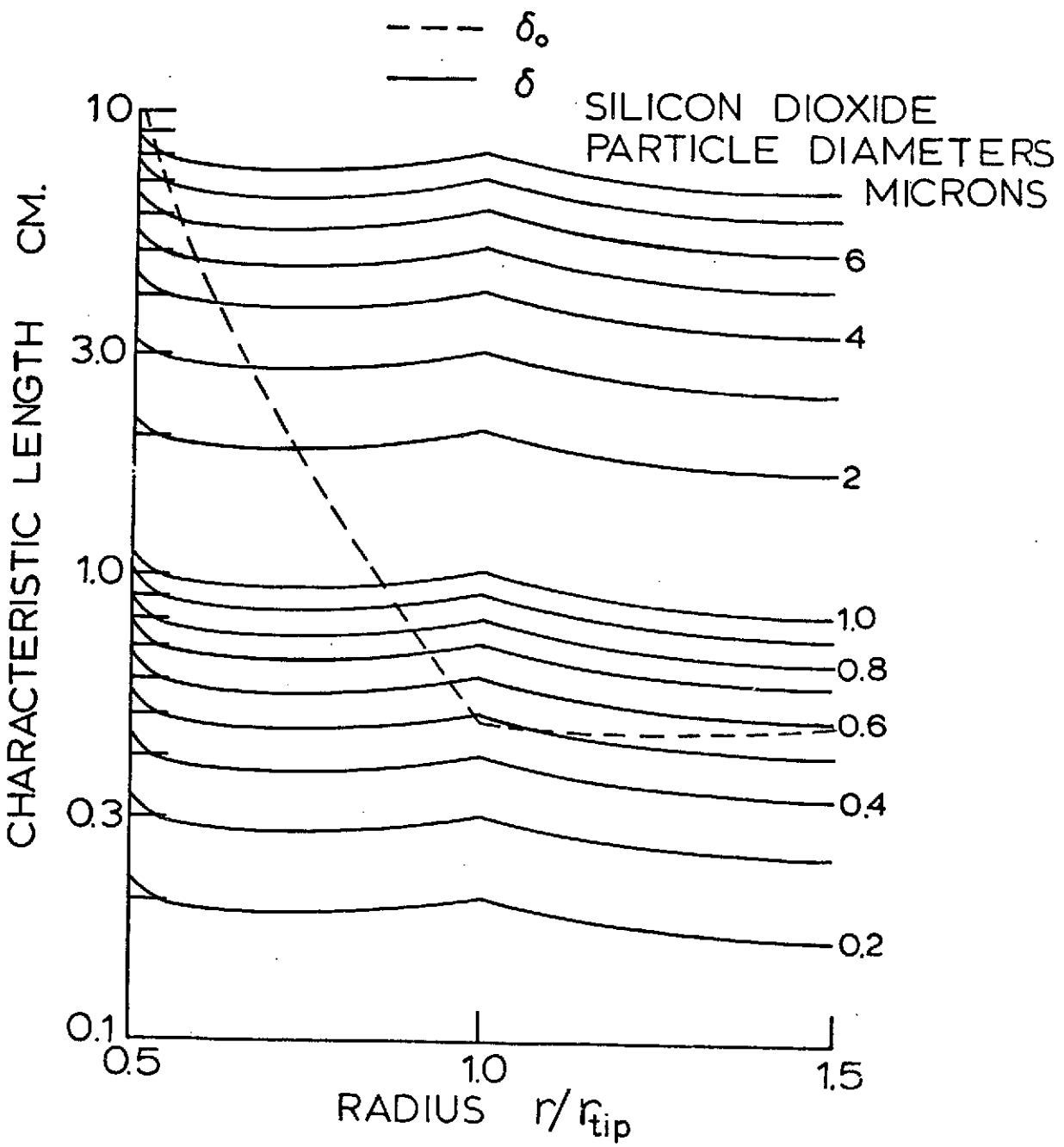

FIGURE 7. CHARACTERISTIC LENGTH VARIATION WITH RADIUS

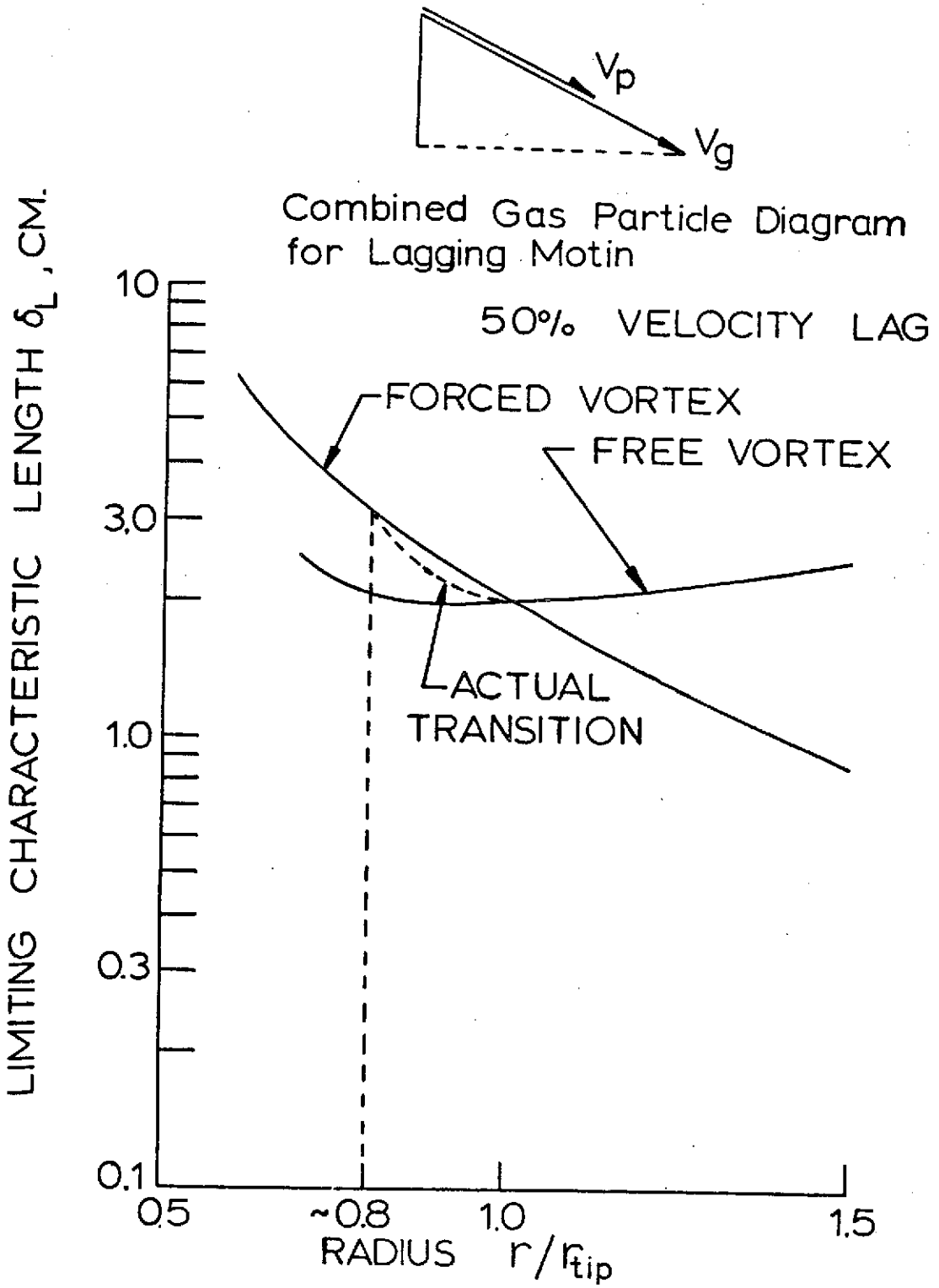

FIGURE 8. LIMITING CHARACTERISTIC LENGTH VERSUS RADIUS

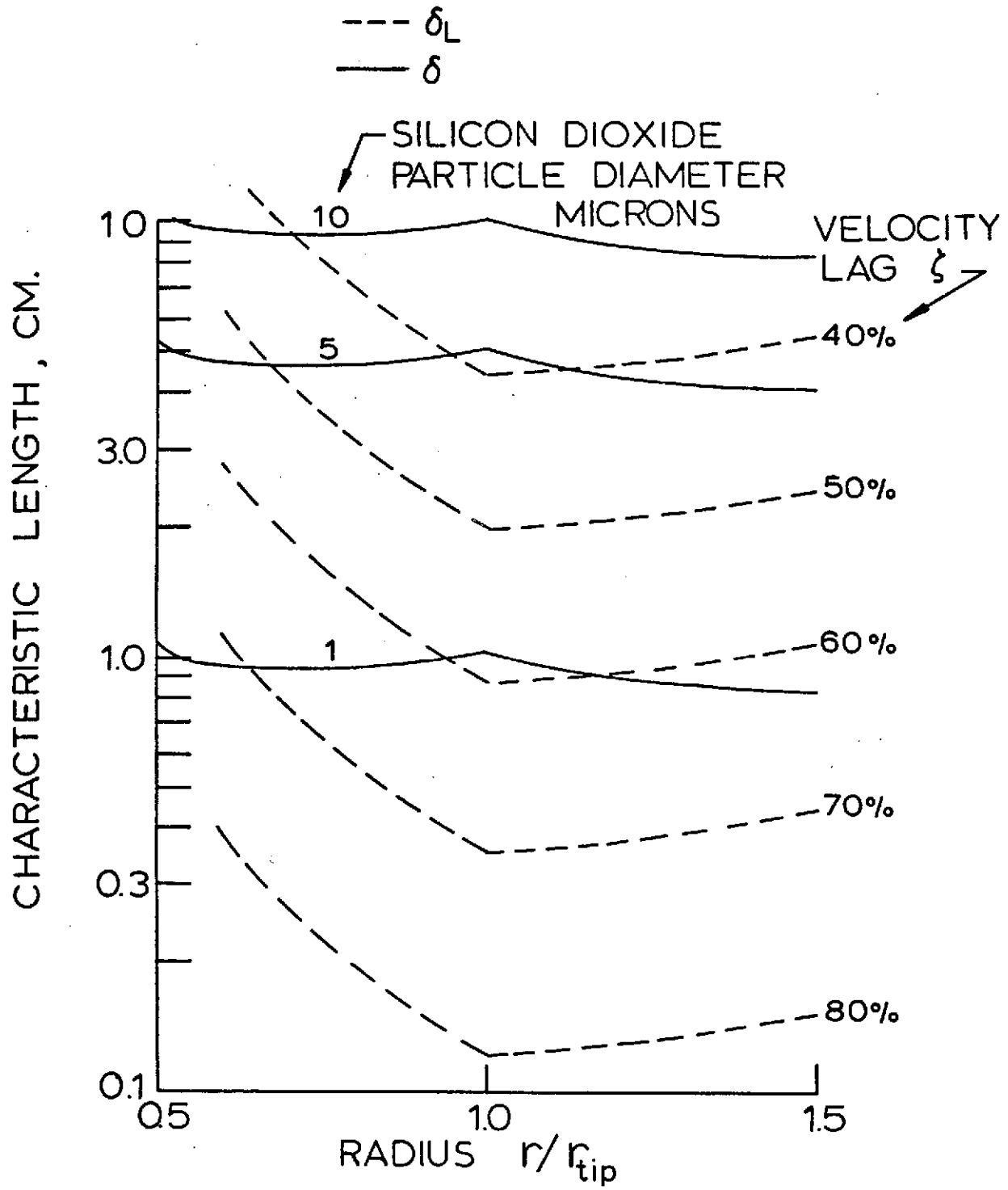

FIGURE 9. CHARACTERISTIC LENGTH VARIATION WITH RADIUS

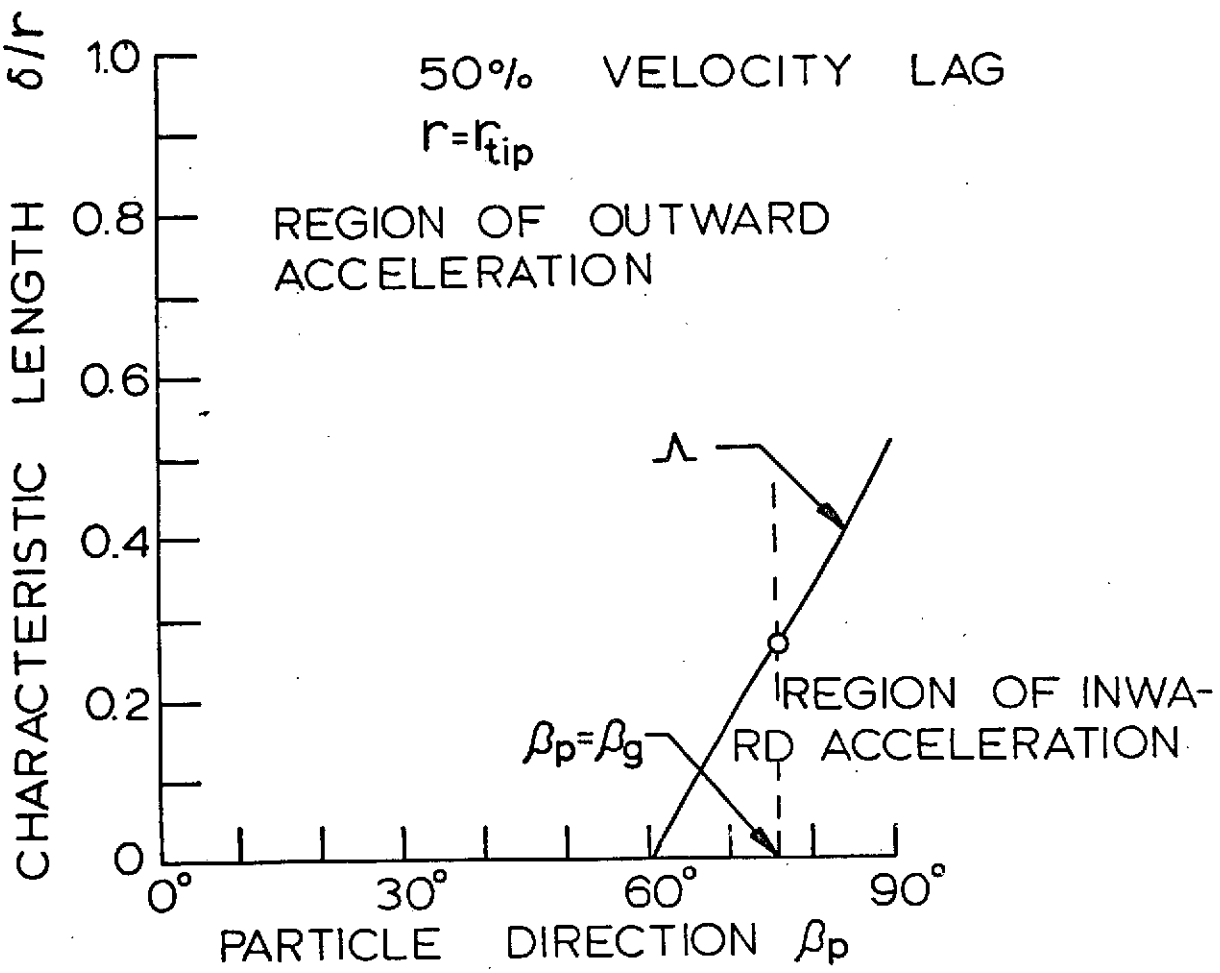

FIGURE 10. ACCELERATION CHART FOR 50% VELOCITY LAG

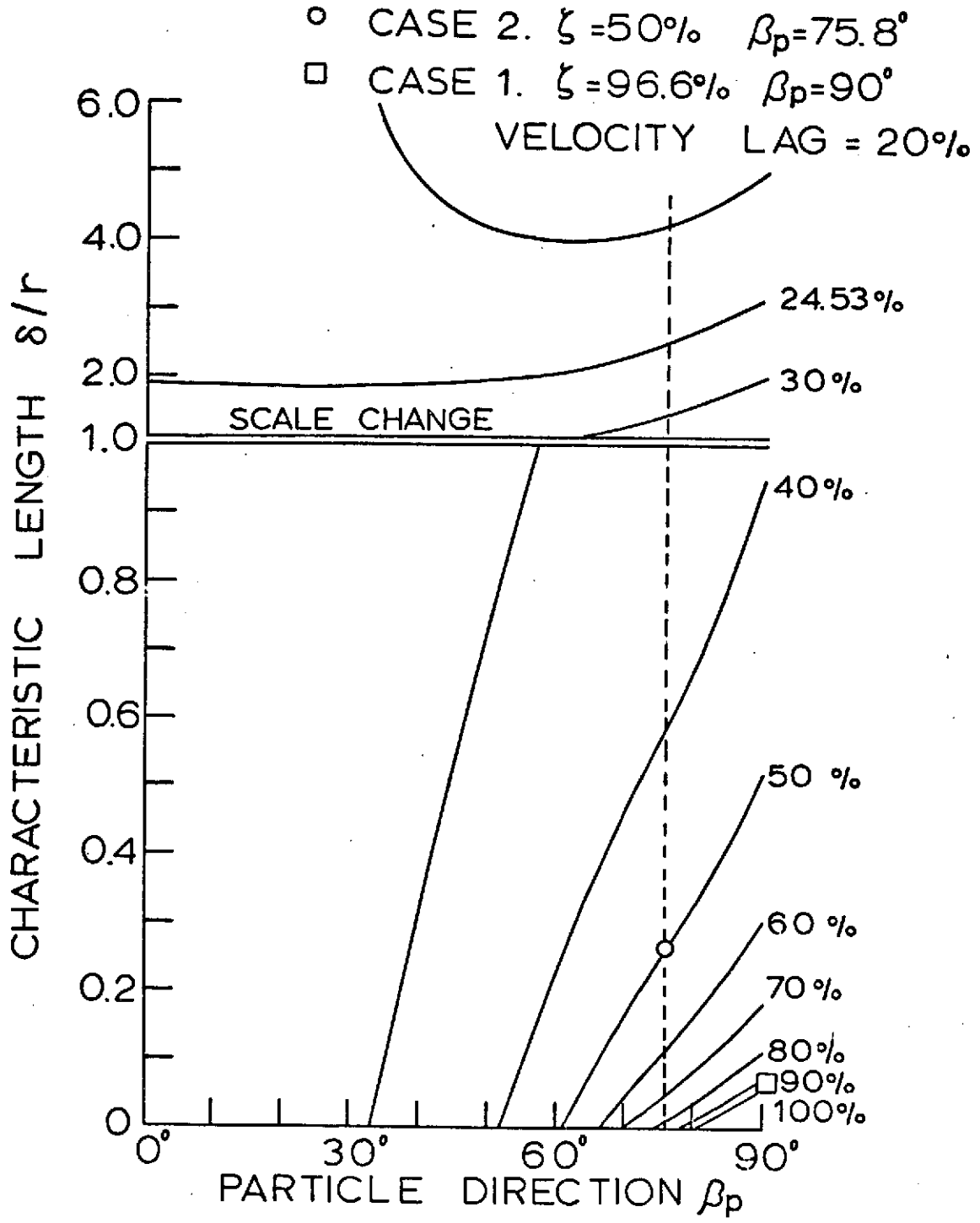

FIGURE 11. ACCELERATION CHART FOR ALL CASES